공학석사 학위논문

Local and Controlled Delivery of Triamcinolone for the Prevention of Fibrosis around Silicone Implants

실리콘 임플란트 주변의 섬유화 예방을 위한 트리암시놀론의 국소적 제어 전달

2018 년 2 월

서울대학교 대학원

협동과정 바이오엔지니어링전공

전 범 수

Abstract

Local and Controlled Delivery of Triamcinolone for the Prevention of Fibrosis around Silicone Implants

Beom Su Jeon
Interdisciplinary Program in Bioengineering
The Graduate School
Seoul National University

I propose silicone implants capable of the local, controlled release of a glucocorticoid drug, triamcinolone acetonide (TA), for the prevention of fibrosis. The shells of these silicone implants were coated with two different loading amounts of TA, which could release the drug in a sustained manner for 12 weeks. The drug-loaded implants were inserted into the subcutaneous space in living rats, and the tissues were biopsied at scheduled times during 12 weeks. For the drug-coated implants, the capsule thickness and collagen density decreased compared with those of the non-coated implant. Because of the effect of TA, inflammation and the expression of pro-inflammatory cytokines, such as TNF-α and IL-1β, were downregulated, thereby decreasing the number of monocytes during acute inflammation. This effect in turn decreased the number of macrophages at the later stage of

inflammation, leading to the expression of less TGF-β and consequently fewer fibroblasts and myofibroblasts. Notably, with an appropriate dose of TA, skin and muscle atrophy, major side effects of TA, could be avoided while still effectively reducing fibrosis. Therefore, I conclude that the local, sustained release of an appropriate dose of a glucocorticoid drug can be a promising strategy for safely preventing fibrosis around silicone implants.

Keywords: Controlled release, Silicone implant, Fibrosis, Inflammation, Glucocorticoid, Triamcinolone

Student Number: 2016–21177

Contents

List of Figures

1. Introduction

1.1 Background knowledge

Silicone implants have been widely used in clinical settings for augmentation mammoplasty and reconstruction surgery [1]; however, this usage has been associated with capsular contracture, which is considered one of the most common and serious complications [2]. Because of capsular contracture, over 10% of patients are required to undergo replacement surgery of the silicone implant, which can increase the financial burden, surgery-related risks and side effects [3].

Capsular contracture is mainly caused by excessive fibrosis, which is the result of an abnormally upregulated and prolonged inflammatory response. In general, after the insertion of a silicone implant, acute inflammation begins with the recruitment of inflammatory cells, such as neutrophils and monocytes, and this recruitment is constantly promoted by cytokines, such as tumor necrosis factor-α (TNF-α), interleukin-1β (IL-1β) and other signal factors released from the tissues around the implant [4-6]. Because of the constant presence of the silicone implant, the inflammatory response enters the chronic stage, in which monocytes are differentiated into macrophages that are responsible for releasing transforming growth factor-β (TGF-β) and other pro-inflammatory cytokines to upregulate the proliferation and activation of fibroblasts [4, 7]. Those fibroblasts synthesize excessive collagen and are also differentiated into myofibroblasts, causing

mechanical tension throughout the peripheral collagenous tissue around the inserted silicone implant and hence inducing capsular contracture [7, 8].

1.2 Strategy

From the perspective of inflammation modulation, glucocorticoids are potentially good candidate drugs for preventing capsular contracture originating from overactive inflammation [9, 10]. Glucocorticoid drugs are known to suppress the overall inflammatory cytokines, including TNF-α and IL-1β, by binding to glucocorticoid receptors and inhibiting transcription factors in inflammatory cells [11-13]. These drugs can also downregulate the expression of chemoattractants and adhesion molecules that are essential for the recruitment of inflammatory cells [9].

Therefore, I hypothesize that the local, sustained delivery of a glucocorticoid drug can prevent fibrosis around a silicone implant. Continuous drug exposure during the period of acute inflammation would suppress the recruitment and activation of polymorphonuclear cells (PMNs) and monocytes. Consequently, fewer macrophages and thus less TGF-β would be produced during the chronic inflammation stage, which in turn would suppress the proliferation and activation of fibroblasts, thereby causing less collagen synthesis [8, 14, 15]. Despite its efficacy, a glucocorticoid drug may cause side effects, such as skin and muscle atrophy [16], especially when the patient is exposed to excess drug. In this sense, accurate control of the dose of

a glucocorticoid drug is important to allow safe treatment for preventing fibrosis.

Therefore, I propose the use of a silicone implant capable of the local, sustained delivery of a glucocorticoid drug, triamcinolone acetonide (TA), to prevent fibrosis. Most importantly, I also pursue to find an appropriate dose of TA that can minimize drug side effects while maintaining the drug's efficacy in inflammation modulation. To meet both aims, therefore, I employed the shells of a silicone implant that is actually in clinical use and coated them with varied drug-loading amounts such that the silicone shell itself could absorb the drug and serve as the controlled-delivery carrier. The coated implant was then inserted in the subcutaneous space of live rats, and the tissue around the implant was biopsied and assessed at scheduled times until 12 weeks after implantation. To determine the *in vivo* drug efficacy in fibrosis prevention, I examined the capsule thickness and degree of inflammation and the collagen density, using hematoxylin and eosin (H&E) and Masson's trichrome (MT) staining, respectively. The inflammatory cells (i.e., monocytes/macrophages, fibroblasts and myofibroblasts) and cytokines (i.e., TNF-α, IL-1β and TGF-β) of interest were analyzed from immunofluorescence (IF)-stained images. To examine the degree of drug side effects, I assessed the thickness of the muscle and skin in tissues around the implant after *in vivo* sample insertion.

2. Materials and Methods

2.1 Materials

The shells of silicone implants in clinical use (BATT-H 295) were generously provided by Hans Biomed (Korea). TA was purchased from Tokyo Chemical Industry (Japan). Acetone and dimethylformamide (DMF) were obtained from DaeJung (Korea) and acetonitrile (ACN) was obtained from J.T. Baker (USA). Medical epoxy (EPO_TEK® 301-2) was purchased from Epoxy Technology (USA). Paraformaldehyde (4%) and isoflurane were supplied by Dreamcell (Korea) and Hana Pharm (Korea), respectively. Xylene, ethanol and acetic acid solution (1%) were purchased from Duksan Pure Chemicals (Korea). Modified Mayer's H&E Y solutions were supplied by Richard-Allan Scientific (USA). Biebrich scarlet-acid fuchsin, phosphomolybdic acid, phosphotungstic acid, aniline blue solutions and hydrochloric acid were obtained from Sigma-Aldrich (USA). Antigen-retrieval solution (10X) and antibody diluent were purchased from Dako (Denmark). Blocking solution (AR-6591-02) was obtained from ImmunoBioScience (USA). VECTASHIELD mounting solution containing 4',6-diamidino-2-phenylindole (DAPI) was purchased from Vector Laboratories (USA). Anti-TGF-ß (sc-146), anti-TNF-α (sc-52746) and anti-IL-1ß (sc-7884) antibodies were obtained from Santa Cruz Biotechnology (USA). Anti-α-SMA (ab5694) and anti-CD163 antibodies were supplied by Abcam (USA) and Bio-Rad (USA), respectively. Secondary antibodies (goat anti-mouse IgG (H+L) cross-adsorbed secondary antibody, Alexa Fluor®

488 (A11001); and goat anti-rabbit IgG (H+L) cross-adsorbed secondary antibody, Alexa Fluor® 594 (A11012)) were purchased from Life Technologies (USA).

2.2 Preparation of silicone implant samples

Using the shells of silicone implants in clinical use (BATT-H 295, Hans Biomed, Korea), I prepared three different implant samples: the shells of intact implant without the drug (IP), those coated with a high dose of TA (TA_IP_H) and those coated with a low dose of TA (TA_IP_L). To prepare the samples, I first cut the shell of silicone implant with a thickness of 1 mm into circular pieces with a diameter of 2 cm. To prepare the IP, the inner surfaces of two intact circular shells were attached using medical epoxy (EPO-TEK® 301-2). To prepare the TA_IP_H and TA_IP_L, solutions of TA at 0.01% w v^{-1} and 0.005% w v^{-1}, respectively, were prepared in acetone and then were sprayed on the outer surface of two circular shells under the following conditions: nozzle orifice: 0.8 mm (Dawon Metal, Korea), spraying pressure: 1.03 bar, sample/nozzle distance: 20 cm; and spraying time: 2 s. The spraying procedure was repeated twice with an interval of 30 min, and then the sprayed sample was dried at 45 °C for 1 h to remove the residual solvent. The inner surfaces of the two drug-sprayed circular shells were then attached with medical epoxy as done with the IP (Figure 1). Thus, all implant samples herein possessed an exposed surface area of 6.28 cm^2.

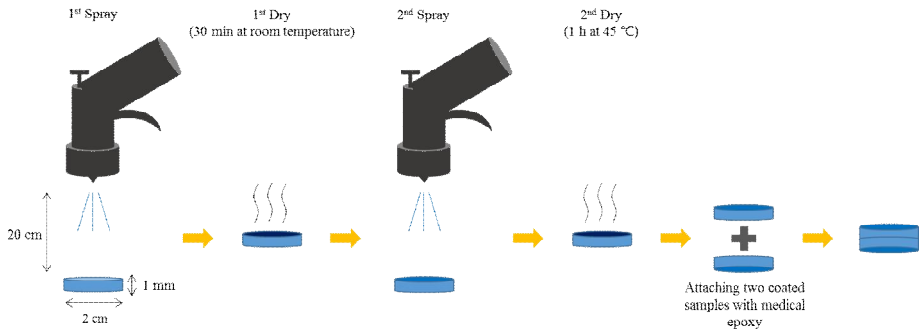

(a)

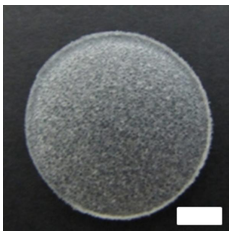

(b)

Figure 1. (a**)** Schematic of the preparation for silicone implant sample. (b) Silicone shell which is cut into circular pieces with a diameter of 2 cm. The scale bar is 0.5 cm.

2.3 Characterization

I imaged the surface of the implant samples with scanning electron microscopy (SEM; 7800F Prime, JEOL, Japan). Prior to this, the samples were sputter-coated with platinum on the SEM sample holder for 1 min (208HR, Cressington Scientific, England). To measure the drug-loading amount in the TA_IP_H and TA_IP_L, I immersed the samples in 5 ml of DMF for a day and then removed and analyzed an aliquot by high-performance liquid chromatography (HPLC; Agilent 1260 series, Agilent Technologies, USA) using a Diamonsil column (C18, 150 x 4.6 mm, 5 μm; Dikma, USA). The mobile phase comprised of a mixture of phosphate-buffered saline (PBS) at pH 2.5 and ACN (1:1, v v^{-1}). The flow rate and injection volume were set at 1 ml min^{-1} and 50 μl, respectively, and the UV absorbance of the sample was measured at 254 nm [17]. And, to ensure that the drug is loaded stably in the TA_IP_H and TA_IP_L, I stretched each of them to 150 % of its original length for 3 min in a 360° twisted state with universal testing machine (UTM; NANOHITECH, Korea) and measure the drug-loading amount of them in the same manner as described above. The experiments were performed in triplicate for each type of sample.

2.4 *In vitro* drug release experiments

I performed the *in vitro* drug release experiments with the TA-loaded implant samples, i.e., the TA_IP_H and TA_IP_L. Each sample was immersed in 5 ml of pH 7.4 PBS, which was placed in a shaking incubator

(SI-600R; Jeio Tech, Korea) at 37 °C with agitation at 125 rpm. At predetermined periods, I collected 5 ml of the release medium and added back to the solution an equal amount of fresh PBS. The obtained media were each tested via HPLC as described above. This experiment was performed in triplicate for each type of sample.

2.5 *In vivo* animal study

To examine the *in vivo* effect of the drug-coated implants, 8-week-old Sprague Dawley (SD) male rats weighing 250 g were used. The animal experiment protocols were approved by the Institute of Animal Care and Use Committee (IACUC) at the Seoul National University Bundang Hospital (BA1608-207/056-01). The animals were raised under specific-pathogen-free (SPF) conditions and were maintained in a 12/12 h light/dark cycle with free access to food and water. In this work, the animals were divided into three distinct groups, which were implanted with the IP, TA_IP_H or TA_IP_L. Five rats were assigned to each of the four different biopsy times, i.e., 2, 4, 8 and 12 weeks after implantation, for a total of twenty rats for each sample type. To insert the sample, hair on the surgery site was removed, and the exposed skin was disinfected with betadine as the rats were anesthetized with isoflurane. Then, the skin was incised, and the implant sample was inserted into a subcutaneous pocket. The skin incision was then closed with a nylon surgical suture (4/0 Nylon B430; WooRiMedical, Korea).

To biopsy the tissues, five rats were selected at the scheduled times after implantation and euthanized using carbon dioxide. The biopsied tissue, which contained the epidermis, dermis, capsule and implant, was fixed in 4% paraformaldehyde and embedded in paraffin. For deparaffinization, the tissue slide was incubated at 60 °C for 1 h to melt the paraffin and was immersed in xylene three times for 5 min each. The animal experiment was performed with the Department of Plastic and Reconstructive Surgery, Seoul National University Bundang Hospital.

2.6 Staining

For H&E staining, the tissue slide was placed into 100%, 95%, 90%, 80% and 70% v v^{-1} ethanol solutions sequentially for 5 min to rehydrate. Next, the slide was dipped in a hematoxylin solution for 3-5 min and then was rinsed with deionized water and a mixed solution of HCl and 70% ethanol (1:400, v v^{-1}). The slide was then immersed in eosin Y solution for 1 min and dehydrated with xylene and ethanol.

For MT staining, the tissue slide was immersed in Biebrich Scarlet-Acid Fuchsin solution for 5 min and washed with deionized water. Next, the slide was incubated in working phosphotungstic/phosphomolybdic acid solution for 5 min. The slide was placed in aniline blue solution for 5 min to stain collagen blue and was then immersed in 1% acetic acid solution for 2 min. The slide was dehydrated using xylene and ethanol.

For IF staining, the slide was first incubated in 1X antigen-retrieval solution and microwaved for 15 min. After cooling at room temperature, the slide was washed with pH 7.4 PBS three times for 5 min each. Next, the slide was treated with goat serum solution for 1 h to block nonspecific antigen binding. The slide was then incubated with diluted primary antibodies in a dark chamber overnight. To evaluate TNF-α, IL-1ß and TGF-ß expression, anti-TNF-α, anti-IL-1ß and anti-TGF-ß antibodies were used at dilutions of 1:200, 1:200 and 1:300, respectively. To evaluate monocytes/macrophages, fibroblasts and myofibroblasts, anti-CD163, anti-vimentin and anti-α-SMA antibodies were used at dilutions of 1:200, 1:250 and 1:50, respectively. After that, the slide was incubated with secondary antibodies at a dilution of 1:2000 at room temperature for 1 h. Anti-mouse antibodies were used for TNF-α, monocytes/macrophages and myofibroblasts. Anti-rabbit antibodies were used for TGF-ß, IL-1ß and fibroblasts. Then, the slide was washed thoroughly with PBS and finally stained with DAPI to stain cell nuclei.

2.7 Stained image analysis

To measure the thicknesses of the capsule, skin and muscle and the degree of inflammation, I examined the H&E-stained tissue slides. For the thickness assessment, images were obtained at 40x magnification (BX43, Olympus, Japan), and I measured the thinnest region of the capsule, skin and

muscle from each of the images. I observed the capsule in the region between the lower part of the dorsal subcutaneous muscle and the upper part of the silicone implant [15, 18, 19]. To evaluate the skin thickness, I measured a whole layer that included epidermis, dermis and subcutaneous tissue. For the evaluation of muscle thickness, I measured the layer of dorsal subcutaneous muscle. To assess the degree of inflammation, on each slide, three randomly selected sites adjacent to the silicone implant were observed at 200x magnification [20], and the degree of inflammation was graded semi-quantitatively as none, mild, moderate and severe (i.e., 0, 1, 2 and 3 points, respectively). To analyze the collagen density, I assessed the MT-stained images at 400x magnification. In each image, the area of blue-stained collagen was measured using ImageJ software (ver. 1.47 software, National Institutes of Health, USA). This area was divided by the whole area of the tissue to give a percentile value [15, 21].

The expression levels of TNF-α, IL-1β and TGF-β and the number of monocytes/macrophages, fibroblasts and myofibroblasts were evaluated with the IF-stained images, which were obtained using a florescent microscope (Imager A1; Carl Zeiss, Germany). For each slide, the DAPI image with cell nuclei was merged with the image of the respective antigen factor using AxioVision LE software (Carl Zeiss, Germany). In this work, TNF-α, monocytes/macrophages and myofibroblasts were stained with fluorescein isothiocyanate (FITC), and IL-1β, TGF-β and fibroblasts were stained with Texas red. The expression levels of TNF-α, IL-1β and TGF-β were graded semi-quantitatively as none, mild, moderate and severe (i.e., 0, 1, 2 and 3

points, respectively) from the image obtained at 400x magnification. I counted the cell numbers from the images obtained at 200x magnification for monocytes/macrophages and those obtained at 400x magnification for fibroblasts and myofibroblasts. For each sample type and each biopsy time, five slides were assessed for statistics.

2.8 Statistical analysis

In this study, for statistical analysis, the non-parametric Kruskal-Wallis test was used to compare the thicknesses of the capsule, skin and muscle; collagen density; degree of inflammation; expression levels of TNF-α, IL-1β and TGF-β; and number of monocytes/macrophages, fibroblasts and myofibroblasts in three groups with dependent variables, which included the biopsy time point (2, 4, 8 and 12 weeks) and implant type (i.e., the IP, TA_IP_H and TA_IP_L groups). Then, I compared two of the three groups using the Mann-Whitney U test and Bonferroni correction. All statistical analyses were considered statistically significant at adjusted P-values <0.05.

3. Results

3.1 Implant characterization

I examined the surface morphology of the implant samples prepared herein via SEM. As shown in Figure 2, the surface morphology of the samples did not vary after coating with the drug. For all samples, rectangular wells with a size of 288.9 ± 71.4 μm were clearly observed, as I employed the shells of the textured-type silicone implants in clinical use. For the drug-loaded implant samples, i.e., the TA_IP_H and TA_IP_L, the loading amounts of TA were measured to be 5.2 ± 0.2 μg cm^{-2} and 2.8 ± 0.1 μg cm^{-2}, respectively, to give total loading amounts per sample of 32.7 ± 1.6 μg and 17.4 ± 0.8 μg. And, the drug-loading amounts of samples which were twisted and stretched were maintained at 97.6 percent of original samples; TA_IP_H and TA_IP_L.

I also performed *in vitro* drug release tests with the TA_IP_H and TA_IP_L. As shown in Figure 3, both TA_IP_H and TA_IP_L exhibited a sustained drug release pattern. In this work, I coated the silicone shell by spraying a TA solution prepared in an organic solvent, acetone. Thus, the drug solution was well absorbed into the silicone matrices [22], which could serve as the drug-diffusion mediator. Both samples herein showed an initial burst for the first three days (c.a. 2.9 μg cm^{-2} and 1.5 μg cm^{-2} for the TA_IP_H and TA_IP_L, respectively), which could be attributed to the drug adsorbed near the surface of the implant. Subsequently, the drug was

released continuously at a rate of approximately 0.02 μg cm^{-2} day^{-1} (TA_IP_H) and 0.01 μg cm^{-2} day^{-1} (TA_IP_L) until 12 weeks. Notably, because of the difference in drug-loading amount, the amount of drug released by the TA_IP_H was about twice as much as that released by the TA_IP_L.

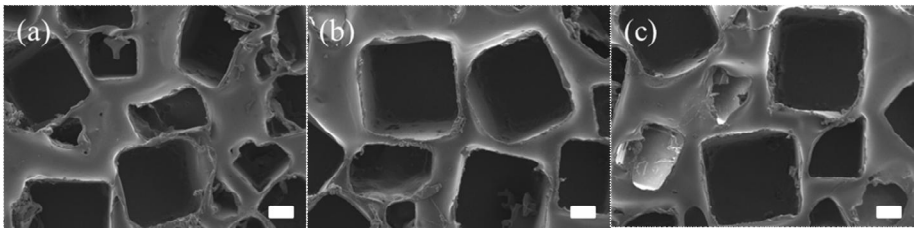

Figure 2. Scanning electron micrographs of the surfaces of the (a) IP, (b) TA_IP_H and (c) TA_IP_L. The scale bars are 100 μm.

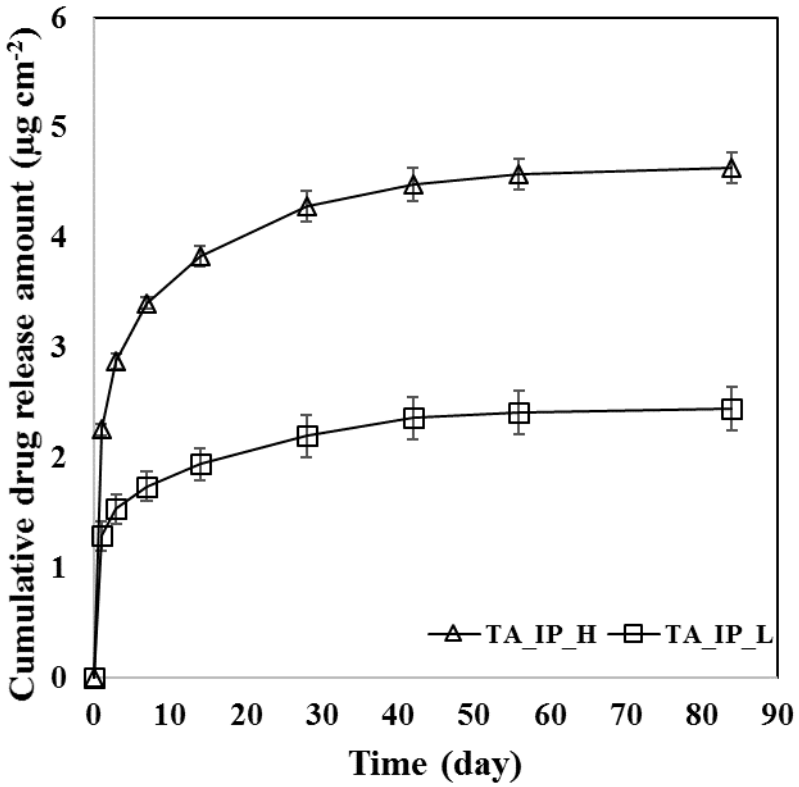

Figure 3. *In vitro* drug release profiles of the TA_IP_H and TA_IP_L.

3.2 Anti-fibrotic effects

To test the *in vivo* efficacy, I first compared the capsule thickness among the three different animal groups (i.e., the IP, TA_IP_H and TA_IP_L groups). As shown in Figure 4, both TA_IP_H and TA_IP_L exhibited reduced capsule thickness compared with the IP, and these differences were statistically significant over the whole testing period ($P < 0.05$). At 12 weeks, the capsule thickness of the IP was 591.0 ± 72.4 μm, which reduced to 430.3 ± 42.3 μm and 379.0 ± 40.2 μm for the TA_IP_H and TA_IP_L, respectively. I also evaluated the collagen density in the capsule, which is known to be one of the important factors in determining the severity of capsular contracture [23, 24]. As shown in Figure 5, compared with the IP, the decreases in the collagen densities of the TA_IP_H and TA_IP_L were again statistically significant during the whole testing period. At 12 weeks, the collagen density of the IP was 76.8 ± 9.8%; by contrast, the collagen densities of the TA_IP_H and TA_IP_L were reduced by more than half to 25.45% ± 10.9 and 30.47 ± 5.5%, respectively ($P < 0.05$). Importantly, the collagen density of the IP continuously increased, as often reported with silicone implants [25, 26]; however, in the presence of TA, the density did not vary but was maintained within the range of 20 - 40%. When I compared the two groups with TA (TA_IP_H and TA_IP_L), the capsule thicknesses and collagen densities were not very different but rather similar, which suggested that the lower dose of TA employed in this work could still have an effect on fibrosis reduction.

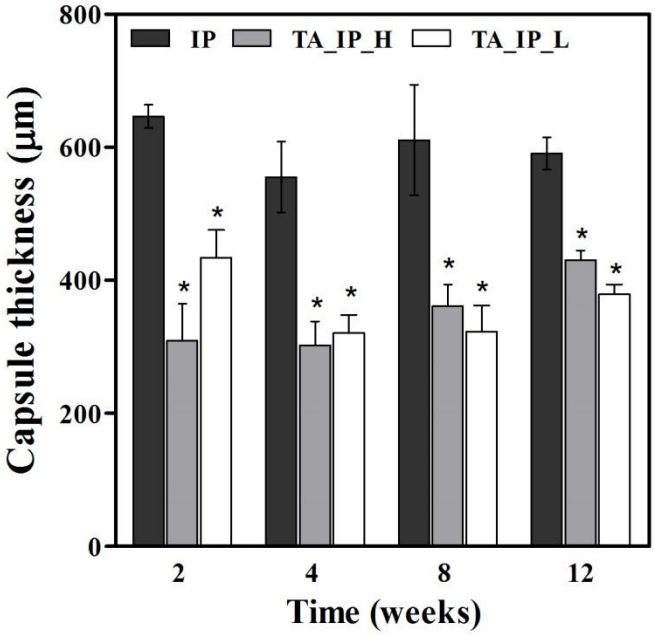

(a)

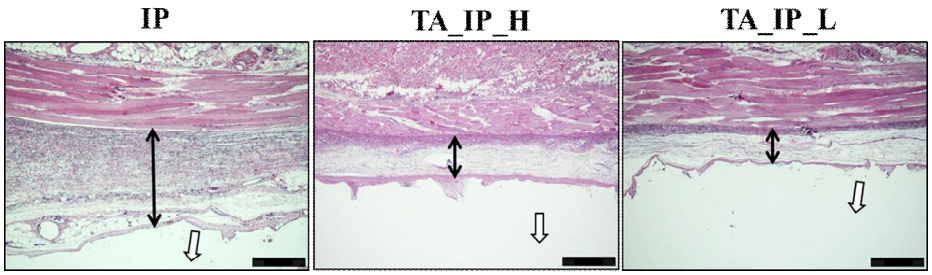

(b)

Figure 4. (a) Profiles of capsule thickness around the silicone implants. The asterisk (*) represents a statistically significant difference compared with the IP ($P < 0.05$). (b) Representative histological images obtained at 12 weeks after implant insertion. The black arrow indicates capsule thickness, and the white arrow shows the location of the implanted sample. The scale bars are 500 μm.

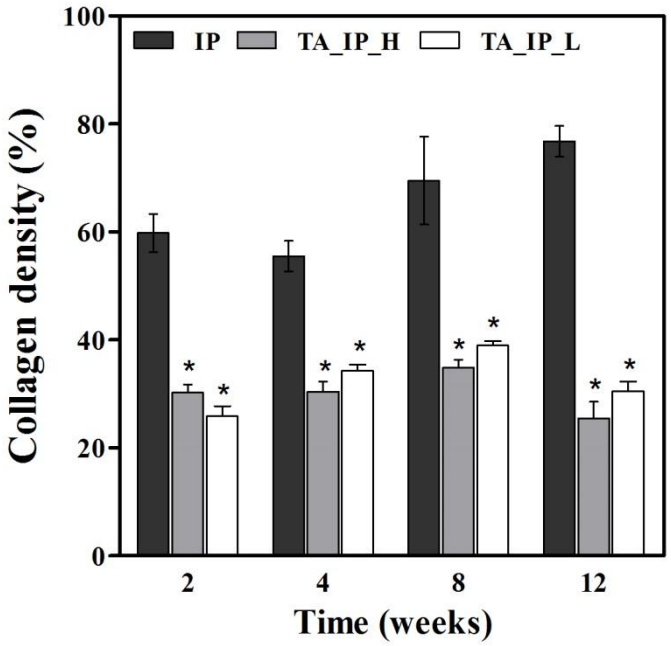

(a)

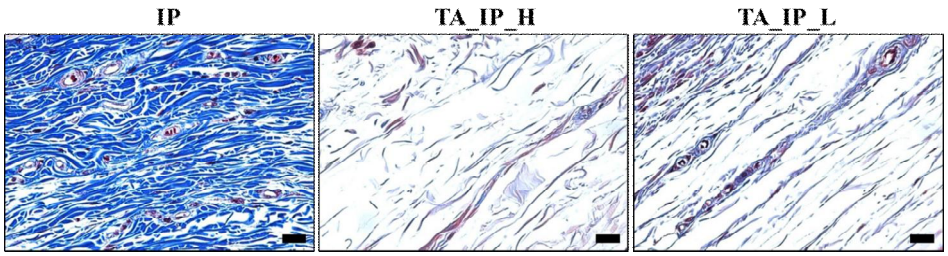

(b)

Figure 5. (a) Profiles of collagen density in the capsule tissue around silicone implants. The asterisk (*) represents a statistically significant difference compared with the IP ($P < 0.05$). (b) Representative histological images obtained at 12 weeks after implant insertion. The scale bars are 20 μm.

3.3 Inflammation

To examine the anti-inflammatory effect of TA, I semi-quantitatively analyzed the degree of overall inflammation based on the number of PMNs [4]. As shown in Figure 6, at 2 and 4 weeks, the degree of inflammation with TA_IP_H and TA_IP_L was statistically significantly lower than that with the IP ($P<0.05$). The IP group exhibited a relatively high degree of inflammation until 4 weeks, which could be ascribed to prolonged acute inflammation that is mostly observed with a nondegradable, bulky implant [14, 27]. During this period, the anti-inflammatory effect of TA therefore appeared to be more prominent. However, from 8 weeks, the difference in the degree of inflammation among the three groups was not apparent because the inflammation was shifted from the acute to the chronic stage, which naturally reduced the number of PMNs, even in the absence of TA [14, 28].

I also evaluated the expression of pro-inflammatory cytokines, such as TNF-α and IL-1β. These cytokines are known to serve as major chemoattractants by recruiting PMNs and monocytes and to be highly involved in the proliferation and activation of fibroblasts [29, 30]. As shown in Figures 7 and 8, both cytokines exhibited significantly lower expression levels with the TA_IP_H and TA_IP_L than with the IP, which, along with the results from the PMNs (Figure 6), further supported the anti-inflammatory effect of TA. The difference was statistically significant at the

period of prolonged acute inflammation, i.e., at 2 and 4 weeks ($P<0.05$) [14, 27].

As one of the important indicators in inflammation, the number of monocytes/macrophages in the capsule tissue was also compared [4, 31]. As shown in Figure 9, throughout the whole testing period, the cell numbers were statistically significantly lower with the TA_IP_H and TA_IP_L than with the IP ($P<0.05$). The stained cells at the early stage (i.e., at 1 – 2 weeks) mostly represented monocytes during prolonged acute inflammation, whereas the cell numbers from 4 weeks originated mostly from macrophages during chronic inflammation [32].

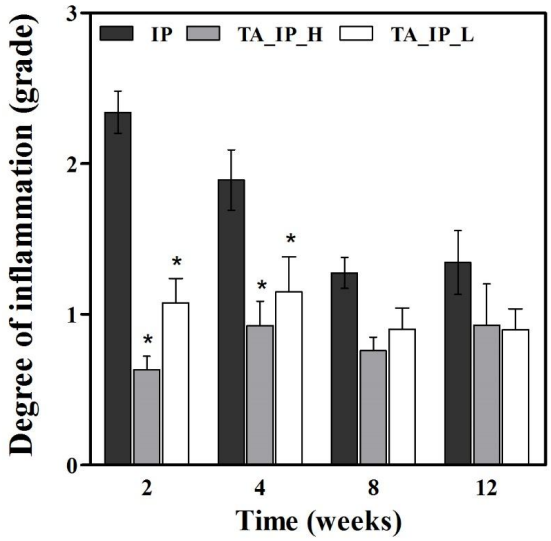

(a)

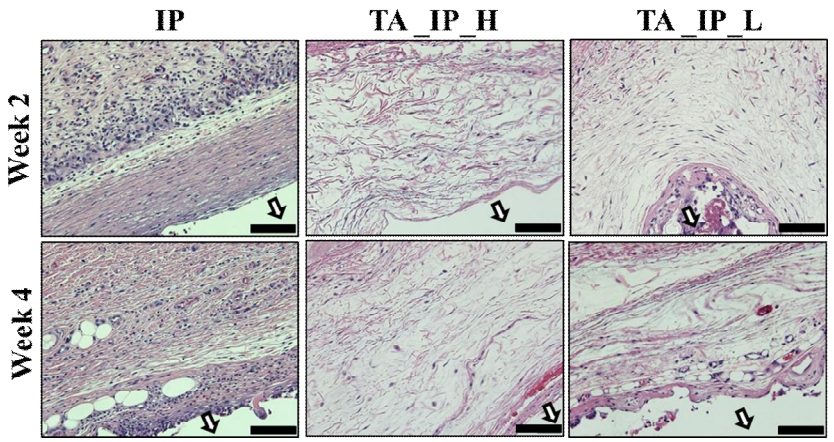

(b)

Figure 6. (a) Profiles of degree of inflammation in the capsule tissue around silicone implants. The asterisk (*) represents a statistically significant difference compared with the IP ($P < 0.05$). (b) Representative histological images obtained at 2 and 4 weeks after implant insertion. The white arrow shows the location of the implanted sample. The scale bars are 100 μm.

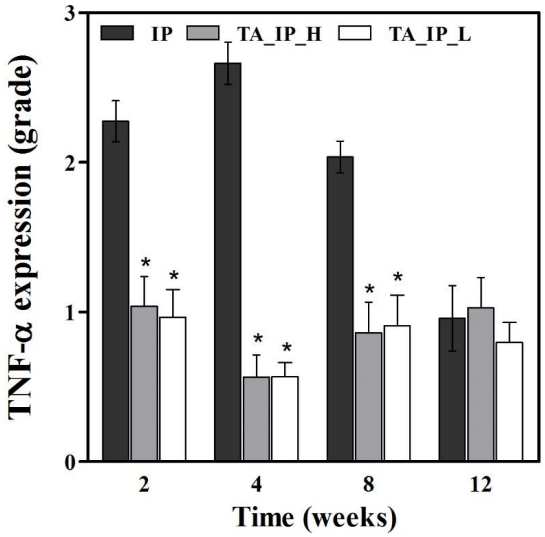

(a)

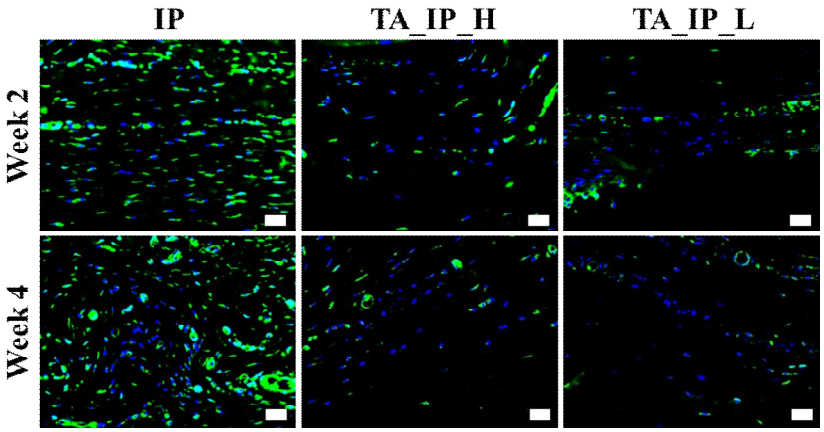

(b)

Figure 7. (a) Profiles of TNF-α expression in the capsule tissue around silicone implants. The asterisk (*) represents a statistically significant difference, compared with the IP ($P < 0.05$). (b) Representative histological images obtained at 2 and 4 weeks after implant insertion. The scale bars are 20 μm.

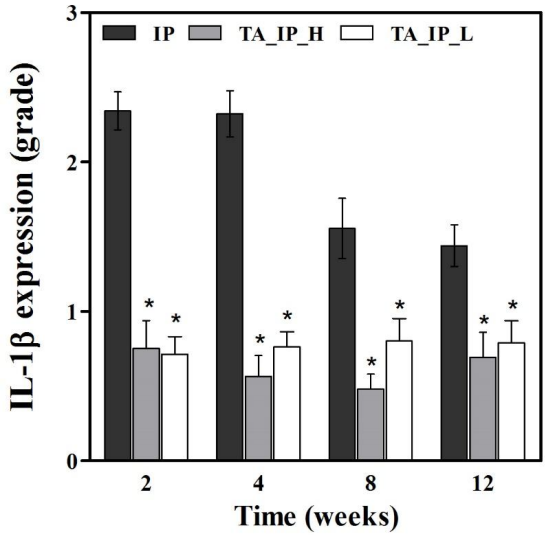

(a)

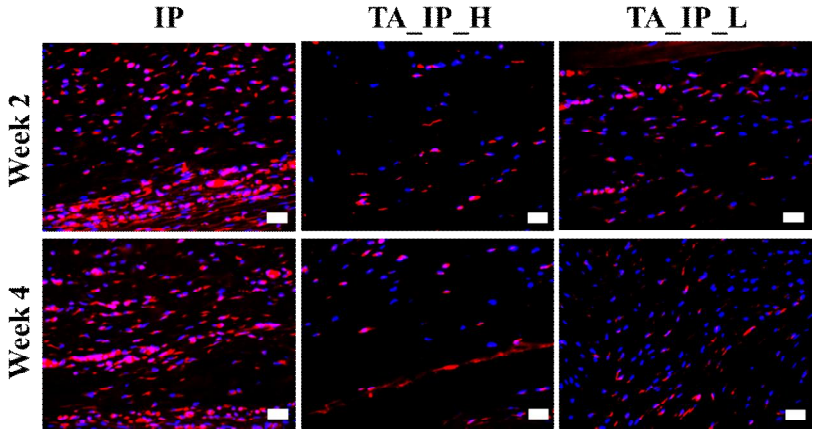

(b)

Figure 8. (a) Profiles of IL-1β expression in the capsule tissue around silicone implants. The asterisk (*) represents a statistically significant difference compared with the IP ($P < 0.05$). (b) Representative histological images obtained at 2 and 4 weeks after implant insertion. The scale bars are 20 μm.

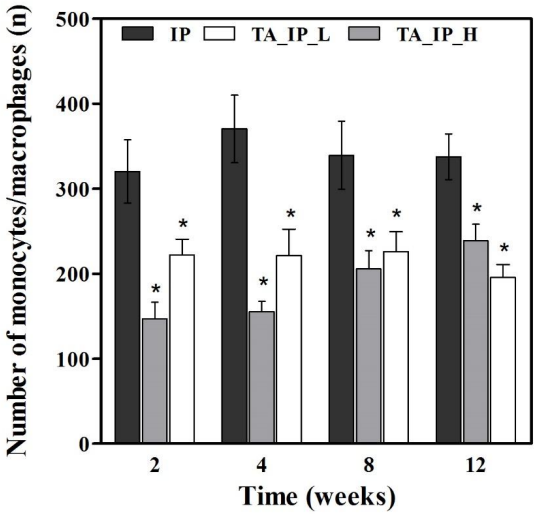

(a)

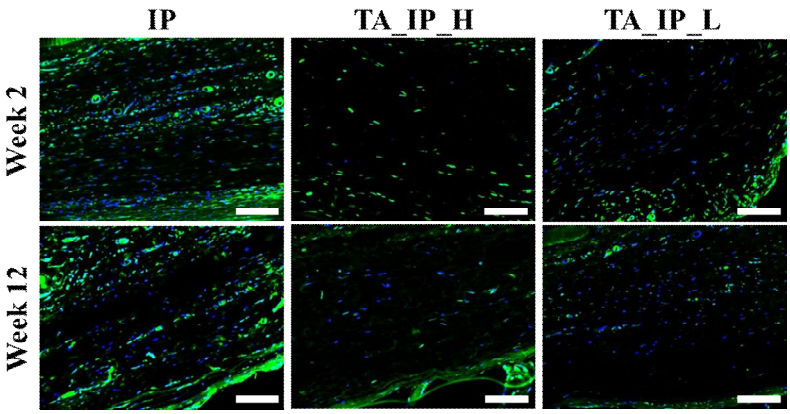

(b)

Figure 9. (a) Profiles of number of monocytes/macrophages in the capsule tissue around silicone implants. The asterisk (*) represents a statistically significant difference compared with the IP ($P < 0.05$). (b) Representative histological images obtained at 2 and 12 weeks after implant insertion. The scale bars are 100 μm.

3.4 Fibrotic factors

I first examined the expression of TGF-β, one of the major cytokines involved in fibrosis. TGF-β induces the expression of α-SMA in fibroblasts and promotes the synthesis and deposition of collagen [33, 34]. Figure 10 shows that relatively high expression of TGF-β was maintained with the IP until 12 weeks; however, this expression level with the TA_IP_H and TA_IP_L was statistically significantly lower ($P < 0.05$). In addition, I evaluated the number of fibroblasts and myofibroblasts. Fibroblasts are a major cell that produces collagen [35, 36] and are known to be differentiated into myofibroblasts, which are responsible for contractile tension around silicone implants [37, 38]. As shown Figures 11 and 12, in the presence of TA, the numbers of both cells were lower than those with the IP. The difference was statistically significant over the whole testing period, except for the fibroblasts at 12 weeks.

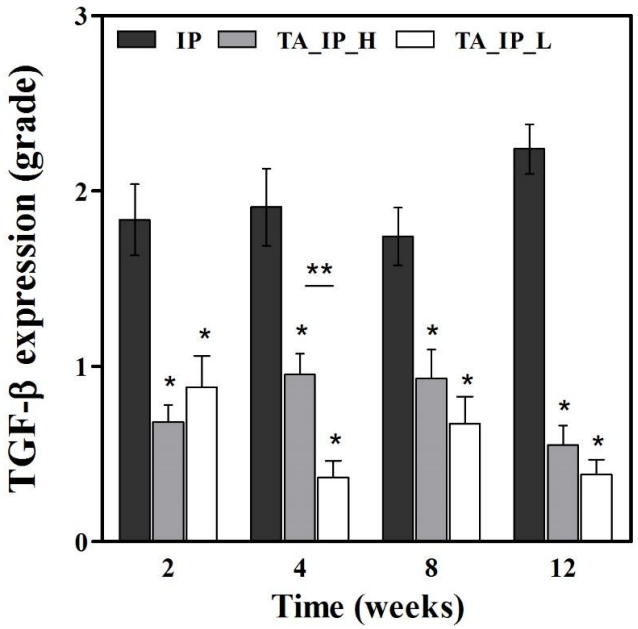

(a)

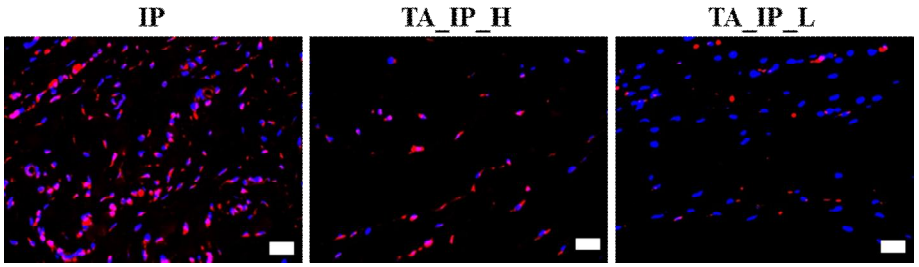

(b)

Figure 10. (a) Profiles of TGF-β expression in the capsule tissue around silicone implants. The asterisk (*) represents a statistically significant difference compared with the IP ($P < 0.05$). Double asterisks (**) represent statistically significant differences between the TA_IP_H and TA_IP_L ($P < 0.05$). (b) Representative histological images obtained at 12 weeks after implant insertion. The scale bars are 20 μm.

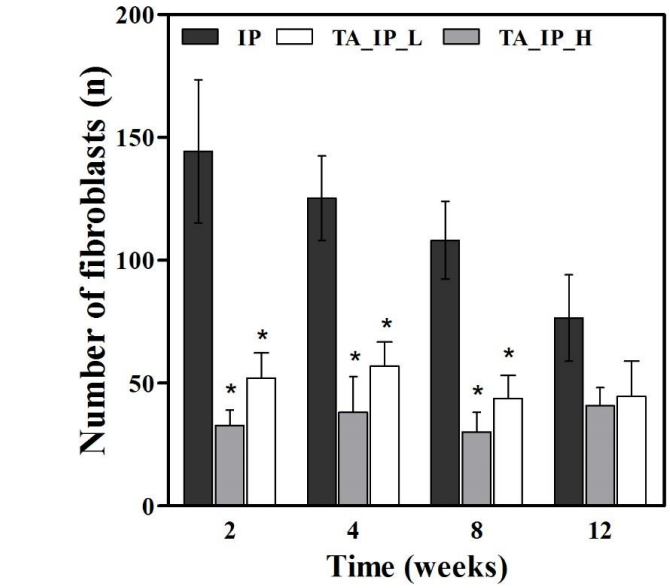

(a)

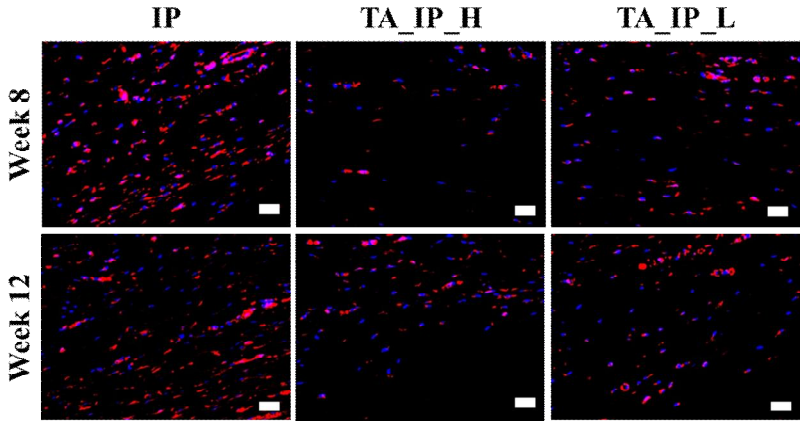

(b)

Figure 11. (a) Profiles of fibroblast number in the capsule tissue around silicone implants. The asterisk (*) represents a statistically significant difference compared with the IP ($P < 0.05$). (b) Representative histological images obtained at 8 and 12 weeks after implant insertion. The scale bars are 20 μm.

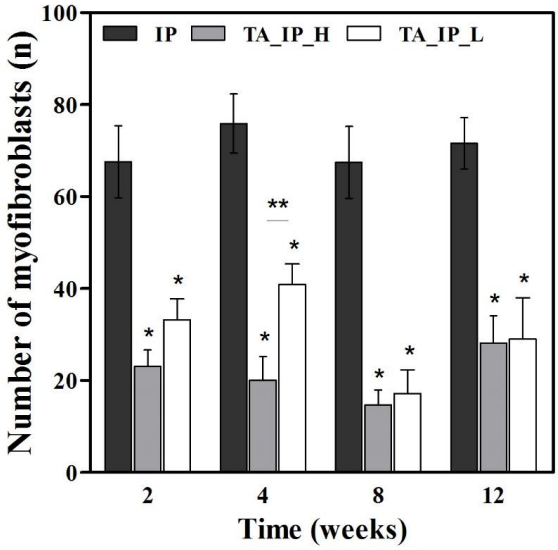

(a)

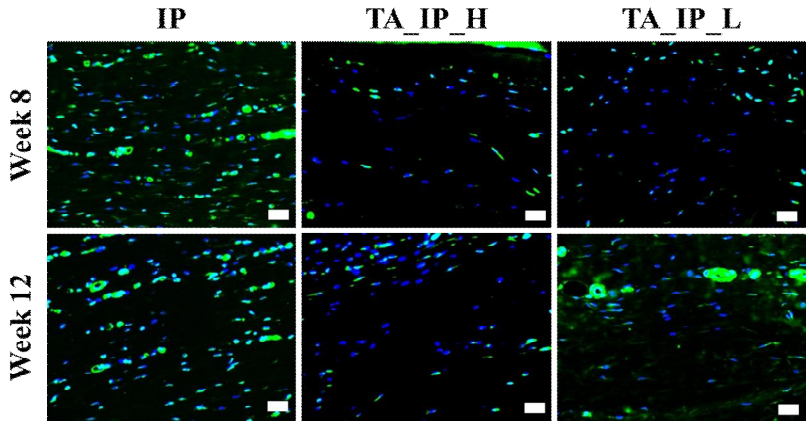

(b)

Figure 12. (a) Profiles of myofibroblast number in the capsule tissue around silicone implants. The asterisk (*) represents a statistically significant difference compared with the IP ($P < 0.05$). Double asterisks (**) represent statistically significant differences between the TA_IP_H and TA_IP_L ($P < 0.05$). (b) Representative histological images obtained at 8 and 12 weeks after implant insertion. The scale bars are 20 μm.

3.5 Drug side effects

When tissue is exposed to an excess amount of TA, the drug is known to cause side effects, such as skin thinning and muscle loss [39, 40]. From the perspective of safety, I investigated therefore the thickness of the skin and muscle above the capsule around the implant (Figure 13). For the IP without TA, the thicknesses of skin and muscle did not vary much until 12 weeks, ranging from 1900 to 2072 μm and from 676 to 782 μm, respectively. However, the TA_IP_H (i.e., the sample with a higher dose of TA) indeed showed a decrease in skin and muscle thickness compared with the IP. Based on my results, the skin thickness appeared to be less affected: it was statistically significantly lower than that of the IP only at 2 weeks but became similar afterwards (Figure 13a). Conversely, the muscle thickness was more severely influenced by the dose of TA. The muscle thickness with the TA_IP_H ranged from 371 to 445 μm, which was statistically significantly lower compared with that of the IP during the whole testing period (Figure 13b). However, when I decreased the dose of TA by half with the TA_IP_L, the thicknesses of both skin and muscle notably remained similar to those with the IP over the whole testing period.

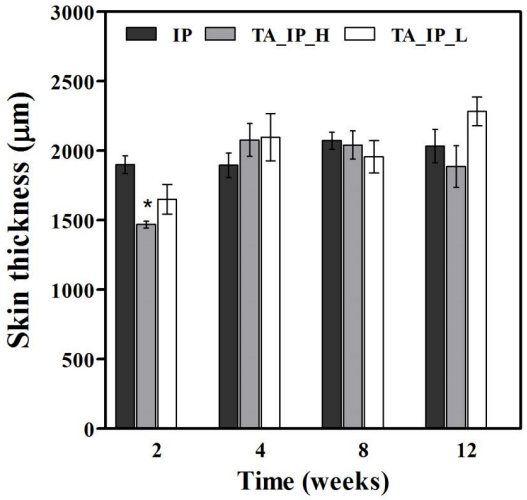
IP
TA_IP_H
TA_IP_L
Skin thickness (μm)
3000
2500
2000
1500
1000
500
0
*
2
4
8
12
Time (weeks)

(a1)

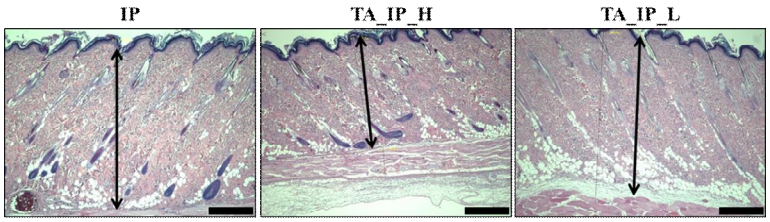
IP
TA_IP_H
TA_IP_L

(a2)

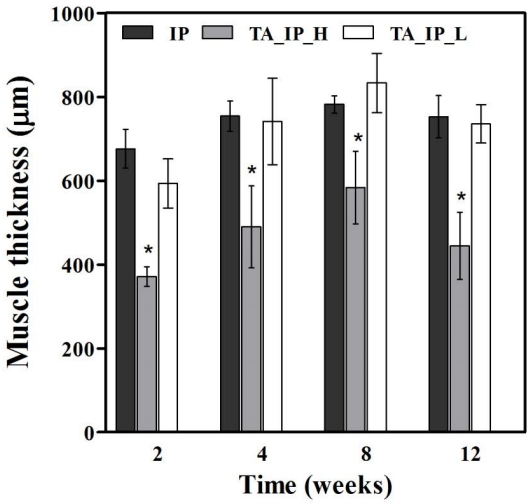

(b1)

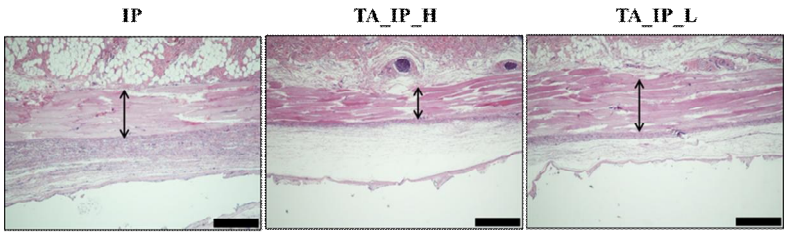

(b2)

Figure 13. Evaluation of drug side effects in the tissue around silicone implants. (a1) Profiles of skin thickness. The asterisk (*) represents a statistically significant difference compared with the IP ($P < 0.05$). (a2) Representative histological images of the skin obtained at 2 weeks after implant insertion. The scale bars are 500 μm. (b1) Profiles of muscle thickness. The asterisk (*) represents a statistically significant difference compared with the IP ($P < 0.05$). (b2) Representative histological images of the muscle obtained at 12 weeks after implant insertion. The scale bars are 500 μm.

4. Discussion

In this work, I propose the use of a silicone implant capable of the local, sustained release of a glucocorticoid drug, TA, to reduce fibrosis. The silicone implant prepared herein could release TA in a sustained manner for up to 12 weeks, which could suppress the pro-inflammatory factors significantly compared with the non-coated, intact implant (Figures 6-10). Consequently, the TA-loaded implants indeed reduced the capsule thickness and collagen density (Figures 4-5), which are the major factors in inducing capsular contracture.

Local, sustained exposure of an anti-inflammatory drug, TA, was observed to significantly lower the degree of inflammation, especially during the period of prolonged acute inflammation (Figure 6). The decrease in the expression of the pro-inflammatory cytokines, such as TNF-α and IL-1β, was prominent (Figures 7 and 8) and in turn reduced the recruitment of inflammatory cells, such as monocytes (Figure 9) [41, 42]. In the transition to chronic inflammation, monocytes are known to differentiate into macrophages [28]. Thus, although drug release was minimal after 4 weeks (Fig. 3), the reduction in macrophages during chronic inflammation could be reflected by the reduced number of monocytes during the earlier stage of inflammation. Macrophages are known to play a key role in secreting TGF-β during chronic inflammation [24]; thus, the reduction in macrophages induced by the TA-loaded implants led to significantly lower expression of TGF-β compared with that of the non-coated, intact implants (Figure 10).

Due to the decrease in TGF-β expression, fewer fibroblasts were observed (Figure 11) [43], and hence, there were fewer of their differentiated cells, myofibroblasts (Figure 12). These cascading events therefore would decrease fibrosis around silicone implants, thereby preventing capsular contracture.

However, over a certain dose, TA can induce problematic side effects, such as skin and muscle thinning [39, 40]. In this work, the implants coated with a higher dose of TA indeed exhibited a significant decrease in skin and muscle thickness (Figure 13). However, when I decreased the dose in the implant by half, the side effects were no longer observed, as almost no difference in skin and muscle thickness was detected compared with the non-coated, intact implant (Figure 13). More importantly, with this controlled dose of TA, the implant still suppressed fibrosis as effectively as the implant with a higher dose of TA. Therefore, my findings suggested the existence of an appropriate therapeutic window of TA level to allow fibrosis prevention without causing significant side effects.

In this work, controlled release of TA could be achieved by a simple combination of the silicone implant and drug without the use of any other materials, as the silicone matrix itself could serve as the drug-diffusion mediator. Thus, the strategy proposed herein could have advantages in the aspects of safety and possibly regulatory approval. In addition, oral administration or injection with a daily dose range up to 40 mg of TA has been already approved for clinical use [44]. In this work, for the TA_IP_L,

an average daily dose was approximately 0.21 μg day^{-1} (Figure 3), which, considering the surface area of silicone breast implants (c.a. 500 cm^2), could be calculated to be approximately 16.5 μg day^{-1} in humans [45]. Therefore, the local dose herein was approximately 2000 times lower than that of conventional TA medications. Albeit proven effective to a large extent, the animal model herein may not be able to fully reflect the condition in human. To be more applicable, therefore, the factors relevant to foreign body reaction, such as tissue trauma due to implant size and surgical procedure, need to be considered further. A longer-term observation after implantation would also provide more information to better support the anti-fibrotic effect with the drug-loaded silicone implant proposed in this work.

5. Conclusion

In this study, I suggest a silicone implant that can release a glucocorticoid drug, TA, in a sustained manner to prevent fibrosis. In addition, I aim at delivering an accurate amount of TA to avoid possible drug side effects, such as skin and muscle thinning. When spray-coated with a TA solution, the silicone implants described herein could release the drug in a sustained manner for 12 weeks with a release rate that could be controlled by the drug-loading amount in the silicone implant. The TA-loaded silicone implants could suppress fibrosis by downregulating overactive inflammation. My *in vivo* experimental results revealed that the drug-coated implants had decreased capsule thickness and collagen density compared with the non-coated implants. This result could be ascribed to the suppression of overall inflammation and pro-inflammatory cytokine expression, thereby reducing the number of fibroblasts and myofibroblasts, which are highly involved in pathogenic fibrosis. Importantly, the silicone implant with an appropriate dose of TA induced almost no change in skin and muscle thickness compared with the non-coated implant while retaining the effect of fibrosis reduction. This result indicated the existence of an appropriate therapeutic window for TA to be applicable for silicone implants in the aspects of both safety and efficacy. Therefore, I conclude that a silicone implant capable of the local, controlled release of a glucocorticoid drug is a promising strategy for preventing capsular contracture.

6. References

[1] M.C. Champaneria, W.W. Wong, M.E. Hill, S.C. Gupta, The evolution of breast reconstruction: a historical perspective, World J. Surg. 36(4) (2012) 730-742.
[2] M. Malahias, D. Jordan, L. Hughes, S. Hindocha, A. Juma, A literature review and summary of capsular contracture: An ongoing challenge to breast surgeons and their patients, Int. J. Surg. Open. 3 (2016) 1-7.
[3] H. Headon, A. Kasem, K. Mokbel, Capsular contracture after breast augmentation: an update for clinical practice, Arch. Plast. Surg. 42(5) (2015) 532-543.
[4] J.M. Anderson, A. Rodriguez, D.T. Chang, Foreign body reaction to biomaterials, Semin. Immunol., 2008, pp. 86-100.
[5] R.S. Cotran, J.S. Pober, Cytokine-endothelial interactions in inflammation, immunity, and vascular injury, J. Am. Soc. Nephrol. 1(3) (1990) 225-235.
[6] S. Wahl, H. Wong, N. McCartney-Francis, Role of growth factors in inflammation and repair, J. Cell. Biochem. 40(2) (1989) 193-199.
[7] X.-m. Meng, D.J. Nikolic-Paterson, H.Y. Lan, TGF-[beta]: the master regulator of fibrosis, Nat. Rev. Nephrol. 12(6) (2016) 325-338.
[8] T.A. Wynn, T.R. Ramalingam, Mechanisms of fibrosis: therapeutic translation for fibrotic disease, Nat. Med. 18(7) (2012) 1028-1040.
[9] D.W. Cain, J.A. Cidlowski, Immune regulation by glucocorticoids, Nat. Rev. Immunol. 17(4) (2017) 233-247.
[10] K.R. Cutroneo, R. Rokowski, D.F. Counts, Glucocorticoids and collagen synthesis: comparison of in vivo and cell culture studies, Coll. Relat. Res. 1(6) (1981) 557-568.
[11] Y. Amano, S.W. Lee, A.C. Allison, Inhibition by glucocorticoids of the formation of interleukin-1 alpha, interleukin-1 beta, and interleukin-6:

mediation by decreased mRNA stability, Mol. Pharmacol. 43(2) (1993) 176-182.
[12] D. Joyce, J. Steer, L. Abraham, Glucocorticoid modulation of human monocyte/macrophage function: Control of TNF-a secretion, Inflamm. Res. 46(11) (1997) 447-451.
[13] R. Schleimer, An overview of glucocorticoid anti-inflammatory actions, Eur. J. Clin. Pharmacol. 45 (1993) S3-S7.
[14] J.M. Anderson, Biological responses to materials, Annu. Rev. Mater. Res. 31(1) (2001) 81-110.
[15] S. Park, M. Park, B.H. Kim, J.E. Lee, H.J. Park, S.H. Lee, C.G. Park, M.H. Kim, R. Kim, E.H. Kim, Acute suppression of TGF-ß with local, sustained release of tranilast against the formation of fibrous capsules around silicone implants, J. Control. Release 200 (2015) 125-137.
[16] H. Schäcke, W.-D. Döcke, K. Asadullah, Mechanisms involved in the side effects of glucocorticoids, Pharmacol. Ther. 96(1) (2002) 23-43.
[17] G.P. Kumar, N. Tirupathirao, T.M. Krishna, RP-HPLC Method Development and Validation for Estimation of Triamcinolone Acetonide in Injectable Suspension using USP-Type-IV Dissolution Apparatus, Int. J. Pharm. Res. Health. Sci. 4(6) (2016) 1504-1509.
[18] R. Ruiz-de-Erenchun, J.D. de las Herrerías, B. Hontanilla, Use of the transforming growth factor-β1 inhibitor peptide in periprosthetic capsular fibrosis: experimental model with tetraglycerol dipalmitate, Plast. Reconstr. Surg. 116(5) (2005) 1370-1378.
[19] P.H. Zeplin, A. Larena-Avellaneda, K. Schmidt, Surface modification of silicone breast implants by binding the antifibrotic drug halofuginone reduces capsular fibrosis, Plast. Reconstr. Surg. 126(1) (2010) 266-274.
[20] P. Nair, H. Duncan, T. Pitt Ford, H. Luder, Histological, ultrastructural and quantitative investigations on the response of healthy human pulps to experimental capping with mineral trioxide aggregate: a randomized controlled trial, Int. Endod. J. 41(2) (2008) 128-150.

[21] B.H. Kim, M. Park, H.J. Park, S.H. Lee, S.Y. Choi, C.G. Park, S.M. Han, C.Y. Heo, Y.B. Choy, Prolonged, acute suppression of cysteinyl leukotriene to reduce capsular contracture around silicone implants, Acta Biomater. 51 (2017) 209-219.
[22] J.N. Lee, C. Park, G.M. Whitesides, Solvent compatibility of poly (dimethylsiloxane)-based microfluidic devices, Anal. Chem. 75(23) (2003) 6544-6554.
[23] W. Dolores, R. Christian, N. Harald, P. Hildegunde, W. Georg, Cellular and molecular composition of fibrous capsules formed around silicone breast implants with special focus on local immune reactions, J. Autoimmun. 23(1) (2004) 81-91.
[24] N. Khalil, O. Bereznay, M. Sporn, A.H. Greenberg, Macrophage production of transforming growth factor beta and fibroblast collagen synthesis in chronic pulmonary inflammation, J. Exp. Med. 170(3) (1989) 727-737.
[25] R.F. Diegelmann, M.C. Evans, Wound healing: an overview of acute, fibrotic and delayed healing, Front. Biosci. 9(1) (2004) 283-289.
[26] E. Minami, I.H.J. Koh, J.C.R. Ferreira, A.F.L. Waitzberg, V. Chifferi, T.F. Rosewick, M.D. Pereira, P.H.N. Saldiva, L.F.P. de Figueiredo, The composition and behavior of capsules around smooth and textured breast implants in pigs, Plast. Reconstr. Surg. 118(4) (2006) 874-884.
[27] M. Schillinger, M. Exner, W. Mlekusch, H. Rumpold, R. Ahmadi, S. Sabeti, W. Lang, O. Wagner, E. Minar, Acute-phase response after stent implantation in the carotid artery: association with 6-month in-stent restenosis, Radiology 227(2) (2003) 516-521.
[28] S.A. Eming, T. Krieg, J.M. Davidson, Inflammation in wound repair: molecular and cellular mechanisms, J. Invest. Dermatol. 127(3) (2007) 514-525.

[29] M. Kolb, P.J. Margetts, D.C. Anthony, F. Pitossi, J. Gauldie, Transient expression of IL-1β induces acute lung injury and chronic repair leading to pulmonary fibrosis, J. Clin. Invest. 107(12) (2001) 1529.
[30] K. Zhang, M. Gharaee-Kermani, B. McGarry, D. Remick, S.H. Phan, TNF-alpha-mediated lung cytokine networking and eosinophil recruitment in pulmonary fibrosis, J. Immunol. 158(2) (1997) 954-959.
[31] C. Shi, E.G. Pamer, Monocyte recruitment during infection and inflammation, Nat. Rev. Immunol. 11(11) (2011) 762.
[32] R.B. Johnston Jr, Monocytes and macrophages, N. Engl. J. Med. 318(12) (1988) 747-752.
[33] I.E. Fernandez, O. Eickelberg, The impact of TGF-β on lung fibrosis: from targeting to biomarkers, Proc. Am. Thorac. Soc. 9(3) (2012) 111-116.
[34] K.M. Hong, J.A. Belperio, M.P. Keane, M.D. Burdick, R.M. Strieter, Differentiation of human circulating fibrocytes as mediated by transforming growth factor-β and peroxisome proliferator-activated receptor γ, J. Biol. Chem. 282(31) (2007) 22910-22920.
[35] D.T. Luttikhuizen, M.C. Harmsen, M.J.V. Luyn, Cellular and molecular dynamics in the foreign body reaction, Tissue Eng. 12(7) (2006) 1955-1970.
[36] T. Wynn, Cellular and molecular mechanisms of fibrosis, J. Pathol. 214(2) (2008) 199-210.
[37] G. Gabbiani, The myofibroblast in wound healing and fibrocontractive diseases, J. Pathol. 200(4) (2003) 500-503.
[38] D.J. Kyle, A. Bayat, Enhanced Contraction of a Normal Breast-Derived Fibroblast–Populated Three-Dimensional Collagen Lattice via Contracted Capsule Fibroblast-Derived Paracrine Factors: Functional Significance in Capsular Contracture Formation, Plast. Reconstr. Surg. 135(5) (2015) 1413-1429.
[39] O. Schakman, S. Kalista, C. Barbé, A. Loumaye, J.-P. Thissen, Glucocorticoid-induced skeletal muscle atrophy, Int. J. Biochem. Cell Biol. 45(10) (2013) 2163-2172.

[40] S. Schoepe, H. Schäcke, E. May, K. Asadullah, Glucocorticoid therapy-induced skin atrophy, Exp. Dermatol. 15(6) (2006) 406-420.
[41] A. Mantovani, The chemokine system: redundancy for robust outputs, Immunol. Today 20(6) (1999) 254-257.
[42] M. Rajesh, P. Mukhopadhyay, S. Bátkai, G. Haskó, L. Liaudet, J.W. Huffman, A. Csiszar, Z. Ungvari, K. Mackie, S. Chatterjee, CB 2-receptor stimulation attenuates TNF-α-induced human endothelial cell activation, transendothelial migration of monocytes, and monocyte-endothelial adhesion, Am. J. Physiol. Heart Circ. Physiol. 293(4) (2007) H2210-H2218.
[43] A. Leask, D.J. Abraham, TGF-β signaling and the fibrotic response, FASEB J. 18(7) (2004) 816-827.
[44] L.M. Sconfienza, C. Murolo, S. Callegari, M. Calabrese, E. Savarino, P. Santi, F. Sardanelli, Ultrasound-guided percutaneous injection of triamcinolone acetonide for treating capsular contracture in patients with augmented and reconstructed breast, Eur. Radiol. 21(3) (2011) 575-581.
[45] G. Catanuto, A. Spano, A. Pennati, E. Riggio, G.M. Farinella, G. Impoco, S. Spoto, G. Gallo, M.B. Nava, Experimental methodology for digital breast shape analysis and objective surgical outcome evaluation, J. Plast. Reconstr. Aesthet. Surg. 61(3) (2008) 314-318.

국문 초록

실리콘 임플란트 주변의 섬유화 예방을 위한 트리암시놀론의 국소적 제어 전달

본 연구에서는 섬유화를 예방하기 위해 글루코코르티코이드 약물인 트리암시놀론 아세토나이드(Triamcinolone Acetonide; TA)를 국소적으로 제어 방출할 수 있는 실리콘 임플란트를 제안한다. 실리콘 임플란트의 쉘(shell)은 2 가지의 서로 다른 양의 TA 를 탑재하도록 각각 코팅되었고, 이것들은 모두 12 주 동안 지속적으로 약물을 방출할 수 있었다. 약물이 탑재된 임플란트들은 살아있는 쥐의 피하 공간에 삽입되었고, 그 조직들은 12 주 동안 예정된 시간에 생체검사되었다. 그 결과, 약물 코팅된 임플란트의 경우, 조직의 캡슐 두께와 콜라겐 밀도가 약물 코팅되지 않은 임플란트의 경우보다 감소하였다. 또한, TA 의 효과에 의해, 종양괴사인자 알파(TNF-α) 및 인터루킨 1 베타(IL-1β)와 같은 염증 유발성의 사이토카인(cytokine)의 발현과 염증 반응이 하향 조절되었고, 그로 인해 급성 염증 반응 단계에서 단핵 백혈구의 수가 감소되었다. 이 효과는 차례로 염증의 후기 단계에서 대식 세포의 수를 감소시켜, 전환성장인자 베타(TGF-β)의 발현을 적게 하였고, 결과적으로 섬유아세포(fibroblasts)와 근섬유아세포(myofibroblasts)의 발현도 적게

하였다. 특히, 적절한 용량의 TA 를 사용함으로, TA 의 주요 부작용인 피부 및 근육 위축을 피하는 것이 가능하였다. 따라서, 본 연구는 적절한 용량의 글루코코르티코이드 약물을 국소적, 지속적으로 투여하는 것이 실리콘 임플란트 주변의 섬유화를 안전하게 예방하는 것에 있어서 유망한 전략이 될 수 있다는 결론을 내리는 바이다.

주요어: 제어 방출, 실리콘 임플란트, 섬유화, 염증 반응,
글루코코르티코이드, 트리암시놀론
학 번: 2016-21177